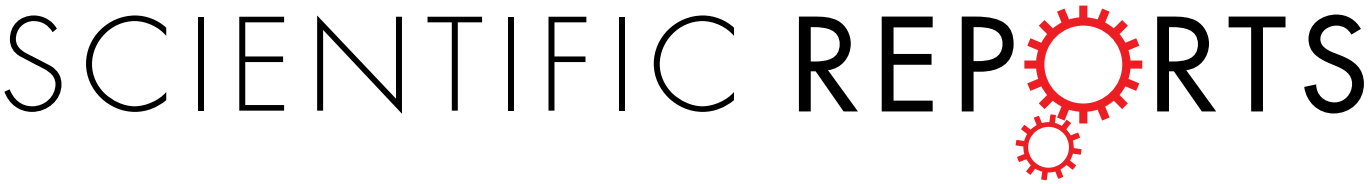

OPEN

Modeling tumor immunity of mouse glioblastoma by exhausted CD8$^+$ T cells

Received: 15 August 2017
Accepted: 12 December 2017
Published online: 09 January 2018

Hiroshi Nakashima[1], Quazim A. Alayo[1], Pablo Penaloza-MacMaster[2], Gordon J. Freeman[3], Vijay K. Kuchroo[4], David A. Reardon[5], Soledad Fernandez[6], Michael Caligiuri[7] & E. Antonio Chiocca[1]

T cell exhaustion occurs during chronic infection and cancers. Programmed cell death protein-1 (PD-1) is a major inhibitory checkpoint receptor involved in T cell exhaustion. Blocking antibodies (Abs) against PD-1 or its ligand, PD-L1, have been shown to reverse T cell exhaustion during chronic infection and cancers, leading to improved control of persistent antigen. However, modeling tumor-specific T cell responses in mouse has been difficult due to the lack of reagents to detect and phenotype tumor-specific immune responses. We developed a novel mouse glioma model expressing a viral epitope derived from lymphocytic choriomeningitis virus (LCMV), which allowed monitoring of tumor-specific CD8 T-cell responses. These CD8 T cells express high levels of PD-1 and are unable to reject tumors, but this can be reversed by anti-PD-1 treatment. These results suggest the efficacy of PD-1 blockade as a treatment for glioblastoma, an aggressive tumor that results in a uniformly lethal outcome. Importantly, this new syngeneic tumor model may also provide further opportunities to characterize anti-tumor T cell exhaustion and develop novel cancer immunotherapies.

Malignant glioma and glioblastoma (GBM) are some of the most common primary central nervous system (CNS) tumors characterized by the accumulation of multiple genetic mutations resulting in uncontrollable cell proliferation and tumor heterogeneity[1]. GBM phenotypes include tumor neovasculature, necrosis, invasion, and immunosuppression. Despite advances in surgery, chemotherapy, and radiotherapy, these cancers result in a uniform mortality, with survival at five years from diagnosis being exceedingly rare[1]. Recent advances in the understanding of how immune responses are regulated during chronic viral infection have led to the discovery of several inhibitory pathways that regulate CD8 T cell effector functions[2–5], and this has translated into novel treatments for solid tumors. Although the central nervous system (CNS) was once thought to be an immune privileged organ, it is now evident that immune cells can infiltrate the CNS to control pathogens and cancers[6–8]. Several immunotherapeutic approaches are being tested for the treatment of GBMs, including CAR-T cells, peptide/nucleic acid vaccination, immune checkpoint blockade, oncolytic and gene therapy, monoclonal antibodies targeting co-stimulatory pathways, and adoptive cell therapies[9–12].

Adaptive immunity against tumors depends on cytotoxic CD8$^+$ T lymphocytes (CTLs) to control and eliminate cancer cells in a durable manner. However, when CTLs infiltrate into the tumor, several immunosuppressive pathways may hinder tumor rejection[13–15]. For example, T cell activation becomes inhibited by immune checkpoint signaling pathways, such as PD-1/PDL-1 and others[2,16,17], leading to T-cell exhaustion[2–5]. Recent studies suggest that these signaling pathways contribute to GBM[18–22] and clinical trials are testing the ability of immune checkpoint inhibitors to treat these aggressive cancers. Seminal studies in the mouse model of chronic LCMV

[1]Harvey W. Cushing Neuro-oncology Laboratories (HCNL), Department of Neurosurgery, Harvard Medical School and Brigham and Women's Hospital, Boston, MA, 02115, USA. [2]Department of Microbiology-Immunology, Feinberg School of Medicine, Northwestern University, Chicago, IL, 60611, USA. [3]Department of Medical Oncology, Dana-Farber Cancer Institute, and Brigham and Women's Hospital, Boston, MA, 02115, USA. [4]Evergrande Center for Immunologic Diseases, Harvard Medical School and Brigham and Women's Hospital, Boston, MA, 02115, USA. [5]Center for Neuro-Oncology, Dana-Farber Cancer Institute, and Brigham and Women's Hospital, Boston, MA, 02115, USA. [6]Center for Biostatistics, The Ohio State University, Columbus, Ohio, 43210, USA. [7]Comprehensive Cancer Center, and Division of Hematology in Department of Internal Medicine, College of Medicine, The Ohio State University, Columbus, Ohio, 43210, USA. Correspondence and requests for materials should be addressed to H.N. (email: HNakashima@bwh.harvard.edu) or E.A.C. (email: EAChiocca@bwh.harvard.edu)

infection revealed that treatment with PD-1 (or PD-L1) blocking antibodies results in significant improvement in T cell function and enhanced antiviral control[2]. These initial findings were soon generalized to various tumor models in mice, and currently PD-1 blockade constitutes a treatment for many types of cancers in humans. This is thought to be also relevant for aggressive cancers, including GBM where CD8 T cells could become dysfunctional due to chronic exposure to tumor antigens[9,23–26]. Several transplantable and genetically engineered preclinical mouse models of GBM exist, where tumors have a relatively limited time frame to grow and establish. This limited time frame may render difficult the chronic presentation of tumor antigens, necessary to induce the "exhaustion" of CTLs. This may potentially magnify the success of tested immunotherapies without recognizing the "true" state of immunocompromise[27]. We thus hypothesized that a previously published model of CTL "exhaustion" that occurs in mice during a chronic LCMV infection could be adapted to recapitulate this dysfunctional state of anti-tumor T-cell immunity in mice models of GBM[2,3,28,29].

Here we show that mice chronically infected with a chronic LCMV strain (Clone 13; Cl13), which induces T cell exhaustion, are unable to reject orthotopic, syngeneic mouse gliomas that express the LCMV GP33 epitope. In contrast, mice infected with an LCMV strain (Arm) that leads to an acute, self-limited infection that induces functional T cell memory, efficiently reject the same GP33 epitope -expressing glioma cells. The failure to reject mouse glioma tumors correlates with high expression of PD-1 in CTLs of Cl-13 mice. Interestingly, this inability to reject mouse gliomas can be partially reversed by treatment with an antibody against PD-1. Altogether, we develop a novel mouse model of cancer that can be used to model the exhausted state of CTLs in GBM and other cancers, and that can be used to evaluate and discover effective immunotherapies.

Results

Failure to reject glioma cells that express the LCMV GP33 epitope in mice chronically infected with LCMV Cl-13. We hypothesized that sharing the same antigen between a tumor and a chronically infectious virus would permit the establishment of a preclinical mouse model that would mimic dysfunctional T-cell immunity. Such a model may be used to study the impact of pre-existent, yet dysfunctional or "exhausted", host immunity in cancer immunotherapy. The previously published LCMV infection mouse model takes advantage of two different strains of LCMV[2,28]. LCMV Arm sets up an acute infection in mice that is cleared resulting in functional memory $CD8^+$ T cells. On the other hand, LCMV Cl-13 sets up a chronic infection that generates $GP33^+$ $CD8^+$ T cells that express high levels of PD-1 and are functionally exhausted, as early as 9 days after infection[30,31]. At day 20 post-infection, LCMV Arm and LCMV Cl-13 infected mice had approximately equal percentages of activated (CD44+) GP33-specific CD8 T cells (Fig. 1A, *left subplots*). However, these GP33-specific CTLs displayed different phenotypic markers in acute vs chronic infection. $CD127^+CD62L^+$ (central memory) and $CD127^+CD62L^-$ (effector memory) cells were PD-1^{low} in Arm (0.17%), but were rare and $GP33^+$ effector cells display PD-1^{high} (79.8%) in Cl13-infected mice (Fig. 1A, *right subplots*, *left upper quadrants*). These findings agreed with those from previous publications[32,33] showing that Arm infection generated highly functional memory $CD8^+$ T cells, in contrast to Cl13 infection that induced an exhausted PD-1^{high} $CD8^+$ T cell population.

We utilized mice infected with either LCMV Arm or Cl-13 to interrogate how they would respond to an intracerebral challenge with CT2A glioma that expresses the cognate LCMV antigen GP33 (designated CT2A-gp33). CT2A-gp33 glioma cells expressed increased levels of the class I major histocompatibility complex (MHC) molecule H-$2D^b$ and of PD-L1, upon stimulation with IFNα, β, or γ (Fig. 1B). There was no change in the expression of the MHC class II molecule I-A^b. We confirmed that CD8 T cells in LCMV Arm-immune mice recognized CT2A-gp33 cells (Fig. 1C).

Next, we characterized the survival of mice challenged with CT2A-gp33 or CT2A gliomas (Fig. 2A). All of the LCMV Arm-infected mice survived an intracerebral challenge with CT2a-gp33 glioma cells, while none of the LCMV Cl-13 infected mice did (Fig. 2B). As expected, no mice survived a challenge with parental CT2A glioma cells that did not express the cognate LCMV antigen. This indicated that PD-1^{high} expressing CTLs were not functionally effective against the CT2A presenting GP33 epitope in Cl-13 mice.

To characterize these contrasting responses against CT2A-gp33, we performed an *ex vivo* assay with splenocytes derived from Cl13 vs. Arm mice. There was an IFN-γ^+ PD-1^{low} population in CD8 T cells in Arm-immune mice in response to CT2A-gp33 (Fig. 3A). In Arm-immune mice, at day 7 of tumor challenge, there was a significant expansion in $GP33^+$ CTLs among brain-infiltrating lymphocytes compared to Cl13 mice (Fig. 3B). PD-1 expression of these $GP33^+$ CTLs in Cl13 mice was elevated when compared to that in Arm mice (Fig. 3B). CD44 expression on GP33+ CTLs was also down-regulated in Cl13 vs. Arm mice, although there was still some degree of expression in most of these cells (supplementary Figure 1). The observed $GP33^+$ CTL expansion in Arm-immune mice was specific to the brain and was not observed in lymphocytes obtained from spleen or blood after CT2A-gp33 or CT2A tumor challenge (Fig. 3C). To provide evidence that CT2A-gp33 challenge directly elicits effector T cell development against the GP33 epitope in the brain, we challenged naïve *(i.e., not LCMV-infected)* mice. There was also a significant increase in the percentage of IFNγ-expressing T cells in response to the GP33 epitope (comparing CT2A-gp33 vs. CT2A) in brains from non- LCMV infected naïve mice, showing that the GP33 antigen could effectively prime brain-infiltrating $CD8^+$ T cells against CT2A-gp33 gliomas in brain (Fig. 3D). Taken together, we developed a model that allows for the easy tracking, phenotypic characterization and tumor protection evaluation by tumor-specific T cells.

PD-1 blockade rescues mice from CT2A-gp33 glioma challenge in the LCMV Cl13 model. We next interrogated if PD-1 blockade can improve the control of CT2A-gp33 gliomas in mice infected chronically with LCMV Cl-13 (Fig. 4A). One day before tumor challenge, we administered a PD-1 blocking or a control antibody every third day for five times (Fig. 4A). PD-1 blockade resulted in a significant improvement in the survival of Cl13 pre-infected mice challenged with CT2A-gp33, when compared to control treated mice (Fig. 4B). PD-1 blockade was effective only when the GP33 epitope was expressed on CT2A cells. We next characterized PD-1 expression on GP33-specific $CD8^+$

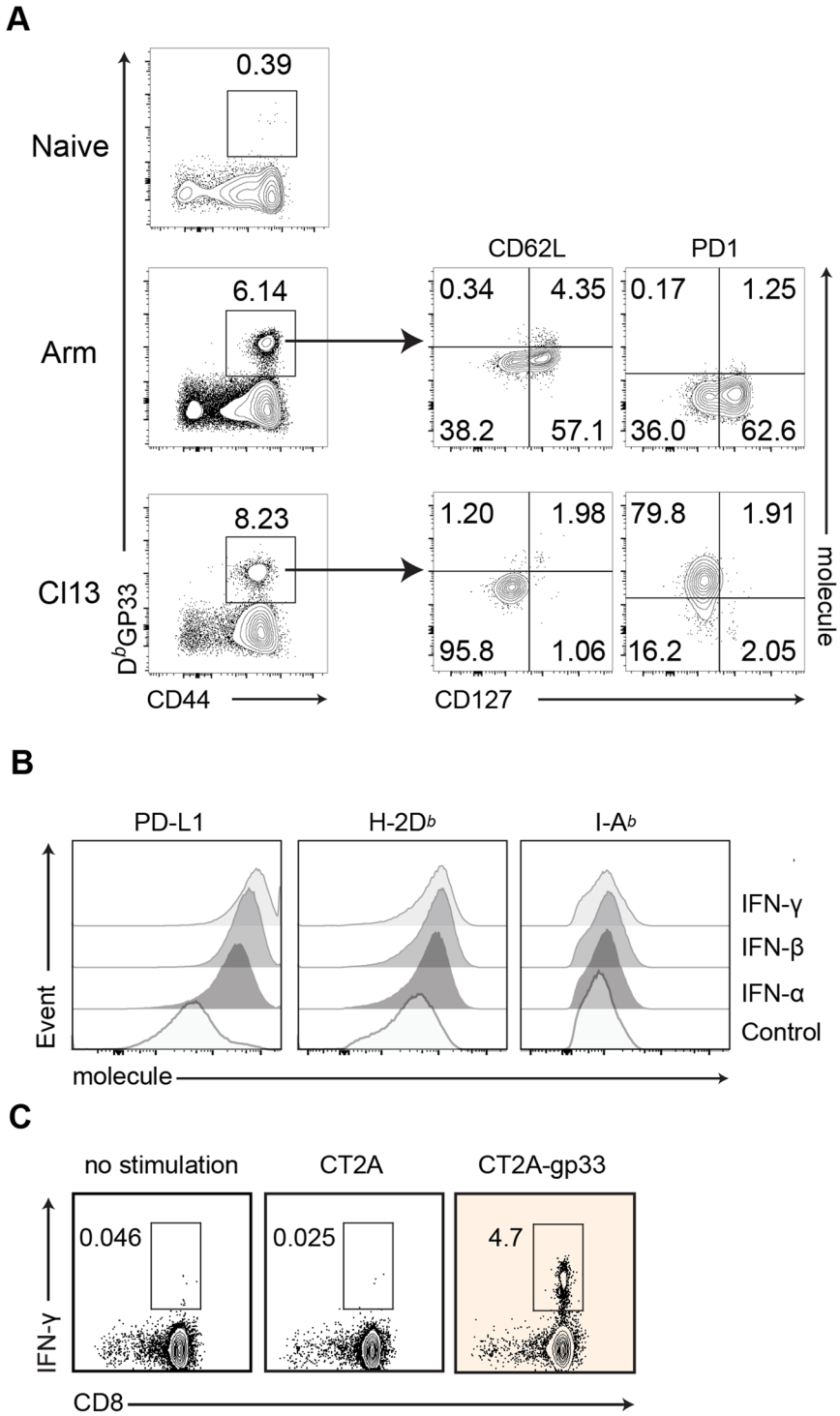

Figure 1. Generation of LCMV GP33 epitope expressing CT2A glioma line and Cl13-induced PD-1^{hi}GP33^{+}CD8^{+} T cells. (**A**) Phenotypic analysis of GP33-specific CD8^{+} T cells in PBMCs of B6 mice infected with LCMV Arm or Cl13, 20 days after infection and before tumor challenge (see Fig. 2 for schematic). The plots are gated on Live^{+}, CD3^{+} and CD8^{+} cells. Molecule on Y-axis *(right subplots)* denotes CD62L or PD-1(labeled top of subplots). Similar results were obtained from mice used in Fig. 2A. (**B**) Histograms showing the frequency of PD-L1, MHC Class I (H-2D^{b}) and II (I-A^{b}) molecules expression on clonal CT2A-gp33 cell populations after exposure to IFN-α, -β (each 500 units/mL) and -γ (20 μg/mL) (**C**) FACS plots showing the frequencies of intracellular IFN-γ expressing CD8^{+} lymphocytes, which were isolated from the spleen of LCMV Arm infected mice after 5 hours of no co-culture (*left*) or co-culture with CT2A (*center*) or CT2A-gp33 (*right*).

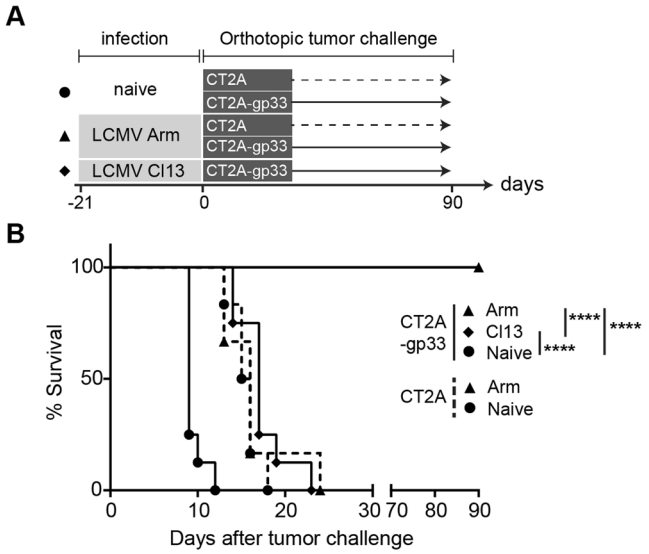

Figure 2. GP33 antigen-dependent rejection of orthotopic gliomas in LCMV Arm-infected, but not Cl13-infected mice. (**A**) Experimental set-up for the orthotopic glioma challenge in LCMV-infected or naive B6 mice. Twenty-one days before tumor challenge, LCMV Arm (acute; *triangle*) or Cl13 (chronic; *diamond*) strain were administered to B6 mice. Age-matched naive B6 mice (*circle*) were used as a comparison. Challenge were glioma cells: CT2A (100,000 cells; *dotted line*) or CT2A-gp33 (400,000 cells; *solid line*) which were implanted into the right brains stereotactically for the survival study (shown in *B*). (**B**) Survival analyses after orthotopic tumor challenge. Survival was monitored for up to 90 days. Median survival after CT2A challenge (n = 6 in each group) was 15 (naive) and 16 (Arm) days, while median survival after CT2A-gp33 challenge (n = 8 in each group) was 9 (naive), >90 (Arm) and 17 (Cl13) days. Log-rank test was used to compare survival among the LCMV infection (Arm, Cl13) and naïve in CT2A-gp33 challenge groups, or between Arm and Naïve in CT2A challenge groups, ****$P < 0.0001$.

T lymphocytes in brains after PD-1 antibody treatment, at 7 and 13 days after tumor challenge. There was a trend for an increase in the numbers of $GP33^{+}CD8^{+}$ T cells in response to PD-1 blockade antibody compared to the isotype control (Fig. 4C). Taken together, these results thus showed that PD-1 blockade rescued the capacity of Cl13-immune mice to reject CT2A-gp33 glioma challenges with an increase in $GP33^{+}$ CTLs. These findings show that PD-1 blockade could be a potent therapy to improve T cell function during both chronic infections and cancers.

Discussion

Tumor recurrence is universal in GBM patients even after standard therapies such as gross total resection and chemo-radiation. The failure of immune surveillance against residual tumor cells is a likely cause for this. One immune evasion mechanism includes the long-term exposure of tumor antigens causing anti-tumor immune cells into a state of progressive dysfunction or exhaustion. Several mouse models where tumors are implanted show evidence that tumor-infiltrating T lymphocytes possess an exhausted phenotype with expression of immune-checkpoint receptors and impaired anti-tumor function[34]. The same T cell phenotypes were initially reported in chronic viral infection using LCMV[2,4,19,33,35,36]. For GBM, a transplantable mouse model using mouse GL261 is commonly utilized, although this model has been criticized for its relatively high immunogenicity that amplifies the outcome of immunotherapy[9,37,38]. Here, we hypothesized that mice with pre-existent exhausted T cell immunity against a specific antigen would not be able to reject a challenge with GBM cells that expressed the same antigen. We show that: **a**- The previously reported model of acute (Arm) vs. chronic (Cl13) LCMV infection could be employed in modeling antigen-specific T cell exhaustion against cancer cells; **b**- This correlated with $PD\text{-}1^{high}$ $GP33^{+}$ T cells in the brains of Cl13 but not Arm mice; and **c**- This lethality was partially but significantly reversed by anti-PD1 treatment. These findings thus show that this mouse model generates consistent $PD1^{high}$-expressing CTLs that do not effectively target a specific antigen for rejection. This is also validated by utilizing PD1 blockade to reverse the phenotype.

One advantage of this model is that tumor establishment occurs in the context of well-defined chronically exhausted T cells that are also found in tumor-infiltrating T-cells in brain (Figs 1 and 3). Systemic LCMV infection elicits a polyclonal $GP33^{+}$ TCR T-cell response that matures from a naïve into an effector phenotype[39]. Therefore, T-cell responses after CT2A-gp33 tumor challenge would reflect the frequencies of pre-existent T cells that accumulate and expand in brains. Our model with LCMV-induced exhaustion in polyclonal T-cell pools against the antigens is comparable to the approach using adoptively transferred T-cells in recipient mice[14,40–42]. This is because specific antigen-specific T cells are traceable and these phenotypes can be manipulated in the donor mice. Despite this advantage in the adoptive T-cell transfer method, tumor-infiltrating lymphocytes appear with heterogeneous phenotypes and in different stages of maturation deriving from the adoptively transferred cells and recipient's T-cell pool that respond to the same specific antigen[40,41]. In the model described in this paper, Cl13 infection-induced $PD1^{high}GP33^{+}$ CTL population become dysfunctional before encountering tumor and thus may

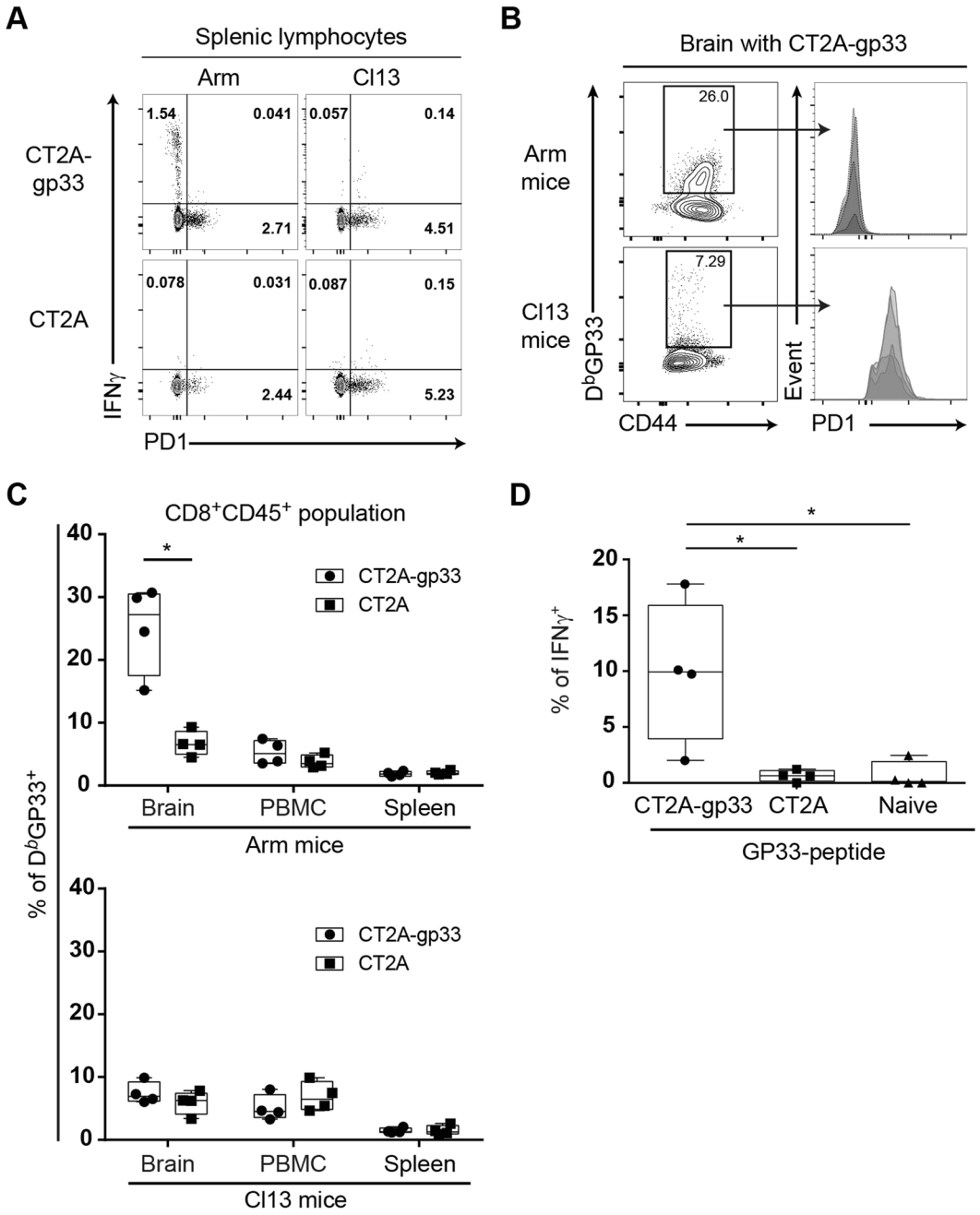

Figure 3. Frequency of GP33 antigen specific CD8+ T cells with PD-1 expression in the brains of Arm vs. Cl13 mice. (**A**) FACS plots showing the frequencies of intracellular IFN-γ and surface PD-1 expressing $CD3^+CD8^+$ T cells at five hours after *ex vivo* co-culture of splenic lymphocytes harvested from mice infected with LCMV Arm (*left*) or Cl13 (*right*), with CT2A-gp33 (*top*) or CT2A (*bottom*). Plot represents one of two replicates. (**B**) Histograms of PD-1 expression of $GP33^+$lymphocytes (*square* in the *left* panel) after gating on $Live^+CD45^+CD8^+$ T cells. Histograms (*right*) of four samples are overlapped while FACS plot (*left*) shows one; (**C**) Percentages of gp33-tetramer positive staining for $CD8^+CD45^+$ cells isolated from brains, PBMC or spleens of Arm- *(upper graph)* or Cl13-preinfected mice at seven days after orthotopic challenge with CT2A-gp33 (*circles)* or CT2A (*squares)*. $GP33^+$lymphocytes are selected as shown in the square in the left panel B after gating on $Live^+CD45^+CD8^+$ T cells. (**D**) Percentages of brain-infiltrating IFNγ -expressing $CD8^+$ T cells, harvested from 7-day old CT2A-gp33 (*left*), CT2A *(center)* or no-tumor control (right) challenged naive (*non LCMV-infected*) mice, 5 hours after *in vitro* incubation with GP33 peptide. Whiskers in box plots indicate maximum and minimum values measured (n = 4; each group), while line indicates the median. Statistical analyses by Student's *t*-test, where $*p < 0.05$.

more closely recapitulate the state of the immune system in advanced stages of cancer, such as recurrent GBM. One limitation of our model may be its mechanistic relevance since the process of antigen-specific T cell "exhaustion" occurs systemically in response to a viral infection and not locally in response to a "true" tumor antigen.

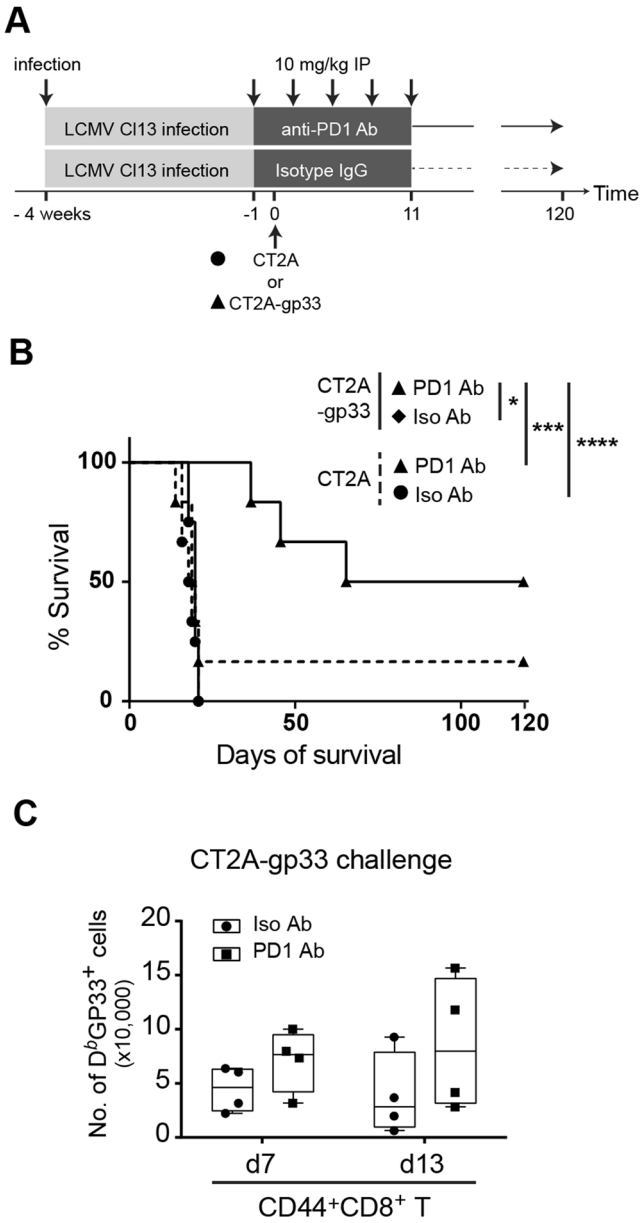

Figure 4. PD-1 blockade restores anti-glioma immunity in Cl13 mice. (**A**) Experimental set-up of the survival study showing the timing of orthotopic glioma challenge and intraperitoneal injections of therapeutic antibodies in LCMV Cl13 infected B6 mice. (**B**) Survival after orthotopic tumor challenge was monitored for up to 120 days. Median survival times after CT2A challenge with anti-PD-1 Ab or its isotype IgG were 20 (n = 4) and 18.5 (n = 6) days, respectively and those after CT2A-gp33 challenge with anti-PD-1 Ab or isotype IgG Ab treatment were 93 (n = 6) and 19.5 (n = 6) days, respectively. Log-rank test was used to compare survival between anti-PD-1 Ab vs isotype IgG in CT2A-gp33 vs CT2A groups, $*p < 0.05$, $***p < 0.001$, $****p < 0.0001$. (**C**) Numbers of GP33-specific effector $CD44^+$ $CD8^+$ T cells in CT2A-gp33-bearing brains of Cl13 pre-infected mice, 7 and 13 days' post-tumor challenge, after treatment with PD-1 antibody or control isotype.

In naïve mouse models[18–22], the effectiveness of PD-1 blockade is observed when the treatment starts early in tumor establishment (usually within the first two weeks of tumor-exposure), possibly because this treatment timing overlaps with the effector phase of primed CTL activation[2,43]. During this phase, these effector T cells are known to express PD-1 to modulate the magnitude of CTL proliferation via apoptosis and this early phase of PD-1 expression during CTL activation is thought to differ from the chronic expression of PD-1 that marks "exhausted" CTLs[2,30,33,42,44–47]. In this study, it appears that our model may mimic this 'exhausted" CTL state even during the early stages of tumor establishment and thus allow for evaluation of immunotherapies (i.e. PD-1 blockade in here) in the presence of exhausted anti-tumor CTLs. Clinical trials of several immune checkpoint inhibitors are currently being pursued. A recent clinical trials using one PD-1 antibody for recurrent GBM patients was reported to show no response in recurrent GBM (NCT02017717) (D.A. Reardon, personal communication)[38]. Another clinical trial for newly diagnosed GBM patients after surgical resection is ongoing (NCT02667587). In

our model, we only saw an effect of PD-1 blockade when it was delivered before and not after tumor challenge. This may imply that the current trials may be mostly effective when tumor burden is minimal, in agreement with other immunotherapy trials[48].

When CTLs infiltrate in the tumor, several immunosuppressive events hinder effective tumor rejection. The tumor immunosuppressive microenvironment is composed of multiple factors, such as regulatory T cells, myeloid-derived suppressor cells, other innate immune cells and cytokines[13–15]. In fact, while we show the blockade of the PD-1 pathway did lead to GBM rejection (Fig. 4B), this protection was not absolute, indicating that effects of PD-1 blockade monotherapy may not completely restore the anti-tumor function of exhausted T cells, possibly because other immune checkpoint signals and epigenetic factors are also operative[2,4,5,33,44,49]. In addition, recent findings show that rescue by PD1-dependent therapies depends on an intact CD28 co-stimulatory pathway[50]. Furthermore, epigenetic programs have also been reported to exert a role in reversion of T cell fate[51]. Although T cells from Cl13-infected mice display the "exhausted" phenotype, it has been shown that they are still able to expand and mount a somewhat effective response, when adoptively transferred into naive mice who are then exposed to an acute LCMV infection[52]. However, we have not yet determined if PD1^{high} *GP33*$^{+}$ T cells from our mice would provide protection to naive mice challenged with CT2A-gp33 gliomas nor have we determined if there are significant differences in the memory compartments of Arm vs. Cl13 mice[51]. The role of these additional pathways in this model remain to be further explored.

We observed that PD-1^{high} GP33^{+} CTL in the brains of Cl13 mice (Fig. 3) could not reject tumor. Instead, Arm mice completely rejected the tumor, if PD-1^{low}GP33^{+} CTLs accumulated in brains (Figs 2B and 3C**; CT2A vs CT2A-gp33**), even though they harbored a similar number of GP33-specific CTL to that of Cl13 mice in the PBMCs (Fig. 1A). To our knowledge, this is novel evidence linking "exhaustion" of CTL to GBM progression. The interaction between cancer and host is thought to lead to "cancer immunoediting," where host immunity gradually shifts from a tumor rejection to a tumor escape role that includes impaired T-cell function and tumor antigen escape[24–26]. An example in GBM is the mutation (R132H) in the IDH1 gene, which can function as an immunogenic antigen initially recognized by CD4^{+} T cells, which then progressively lose their anti-tumor function[53,54]. Short-term (Arm) vs long-term (Cl13) exposure to the gp33 antigen may also skew the development of naïve T cells into memory T-cell vs. non-memory T cells (Fig. 1A). The observed downregulation of CD44 expression in Cl13 may also contribute to the "exhausted" state[55,56] (supplementary Figure 1).

In conclusion, this experimental mouse model should be useful to further characterize the role of dysfunctional immunity in tumor progression.

Materials and Methods

DNA constructs. The immunodominant LCMV epitope GP33-41 was synthesized (IDT, Coralville, Iowa) and cloned in pENTR/D-TOPO (Life Technologies). Inserted sequences were confirmed by DNA sequencing (Eton Bioscience, Boston MA). The fragments inserted between attL1 and attL2 sites were further transferred into the plenti-PGK-puro-DEST vector (addgene, Cambridge MA) using Gateway LR Clonase II kit (Life Technologies). Packaging of lentiviral vectors was conducted in 293FT cells (Life Technologies) by transfecting these constructs with pMD2.G and psPAX2 packaging vectors as described previously[57].

Cell lines. Mouse CT-2A glioma cells were initially generated by Dr. Tomas Seyfried (Boston College, Boston MA) and tested as negative for Mycoplasma infection in the Laboratory of Virology and Epidemiology of Yale University[58]. They were cultured in Dulbecco's Modified Eagle Medium (D-MEM) supplemented with 10% fetal bovine serum (FBS) and 10 mM HEPES (4-(2-hydroxyethyl)-1-piperazineethanesulfonic acid) buffer. All media and supplements were obtained from Thermo Fisher Scientific (Waltham, MA). Cells were infected with the lentiviral vector that encodes the human PGK promoter-driving the LCMV epitope peptide sequences, GP33-41 (GP33: M-KAVYNFATM). The resulting infected cells were diluted and selected using 5 μg/mL puromycin (Sigma) to isolate clonal cell populations that were then analyzed by RT-PCR (data not shown) and T cell proliferation assays to identify the GP33 epitope expressing clones (Fig. 1C). The primers and probes in this study were designed by PrimerQuest Tool (IDT; Coralville, Iowa) as follows: 18 s rRNA (VIC-AGTTGGTGGAGCGATTTGTCTGGT-QSY, 5′-CACGGACAGGATTGACAGATT-3′ and 5′-GCCAGAGTCTCGTTCGTTATC-3′), WPRE (6-FAM-TGCTGACGC/ZEN/AACCCCCACTGGT-IBFQ, 5′-CCGTTGTCAGGCAACGTG-3′ and 5′-AGCTGACAGGTGGTGGCAAT-3′), GP33 (5′-AATTTCGCCACCATGTGAAAG-3′ and 5′-GGGCCACAACTCCTCATAAA-3′). For the T-cell proliferation assay, splenocytes obtained from mice, pre-infected with Arm, were co-incubated with RT-PCR positive clones for 5 hours and subsequently analyzed by fluorescence-activated cell sorting (FACS), as described in Fig. 1C. One of the clones, CTgp33.7 (clone 7), was selected for this study and named CT2A-gp33. After establishing this cell line, expanded cells were cryopreserved to minimize passages (no more than ten) before implanting *in vivo*.

***In vivo* animal studies.** *All e*xperimental procedures using animals were carried out under an animal protocol reviewed and approved by the Harvard Center for Comparative Medicine (HCCM) and BWH's IACUCs, and performed in accordance with relevant guidelines and regulations. C56Bl/6 J mice were purchased from The Jackson Laboratories (Bar Harbor, ME) and infected with LCMV Armstrong by intraperitoneal injection with 2×10^5 pfu or LCMV clone-13 by intravenous injection with 4×10^6 pfu. At 3-weeks after LCMV infection, CT-2A cells (1×10^5 in 5 uL Hank's Balanced Salt Solution or HBSS) and CT2A-gp33 (4×10^5 cells) were injected intracranially at stereotactic coordinates (ventral 3.5, Rostral 0.5 and right lateral 2.0 (in mm) from bregma) using a stereotaxic apparatus (David Korp Instruments; Tujunga, CA). For antibody treatment, PD-1 Ab (29 F.1A12) or isotype control IgG (2A3) were obtained from BioXcell (West Lebanon, NH), diluted in phosphate-buffered saline (PBS) and administered at doses of 10 mg per kg body weight by intraperitoneal injection. Brain tissues

were collected after perfusion with chilled PBS buffer and dissociated with enzyme mixture in RPMI1640 with 5% FBS at the following doses: 30 U/ml of DNase I type IV, 0.1 mg/ml of Hyaluronidase type V, and 1 mg/ml of Collagenase type IV (all from Sigma). After washing dissociated cells with RPMI with 2% FBS, lymphocytes were enriched in the 67–44% Percoll gradient solution (GE Healthcare) at 2,000 rpm for 20 minutes at room temperature. Peripheral blood mononuclear cells (PBMCs) were enriched using Ficoll-Plaque Plus solution (GE Healthcare) at 1,900 rpm for 20 minutes. Single-cell suspensions from spleens were prepared by passing cells through 70-μm cell strainers and Ammonium-Chloride-Potassium (ACK) lysis.

Antibodies and flow cytometry. For surface staining, fluorophore-conjugated mAbs specific for CD3 (17A2), CD44 (IM7), CD279/PD-1 (RMP1-30), CD127 (A7R34), CD62L (MEL-14), H-2D[b] (KH95), I-A[b] (AF6-120.1) were obtained from Biolegend (San Diego, CA), CD45(30-F11), CD274/PD-L1 (MIH5), CD8a (53–6.7) were from BD Biosciences (San Jose, CA). Live/Dead Near-IR Dead cell stain kit, and APC-streptavidin were from Thermo Fisher Scientific (Waltham, MA). For GP33 tetramer staining, the biotinylated class I monomer, obtained from the National Institutes of Health Tetramer Core Facility (Emory University, GA), was conjugated with APC-streptavidin to form the tetramer. For intracellular IFNγ staining, 1×10^7 splenocytes (Figs 1C and 3A) or total number of Percoll-isolated lymphocytes (Fig. 3D) were stimulated at 37 °C for 5 h with 1×10^6 tumor cells or 1 μg/ml GP33-41 peptides (GenScript) in the presence of GolgiStop and GolgiPlug (BD). The cells were washed and surface stained before intracellular staining with anti-IFNγ (XMG1.2) using BD Cytofix/Cytoperm™ Plus solution kit. Cells were run on an LSR II (BD Biosciences) at CCVR Flow Cytometry Core in Beth Israel Deaconess Medical Center (BIDMC; Boston, MA), and analyses were performed with FlowJo (TreeStar).

Statistical analysis. All analyses were completed using the Prism 6 (GraphPad). Unadjusted pairwise comparison p-value for the log-rank test was used for survival analyses (Figs 1C and 3B), and Wilcoxon rank-sum test p-values for comparing treatments or conditions (Figs 2C,D and 3C–E). Kaplan-Meier survival plots and whiskers in box plots were generated with Prism 6 and formatted with Illustrator CS6 (Adobe) Software.

References

1. Brennan, C. W. *et al.* The somatic genomic landscape of glioblastoma. *Cell* **155**, 462–477, https://doi.org/10.1016/j.cell.2013.09.034 (2013).
2. Barber, D. L. *et al.* Restoring function in exhausted CD8 T cells during chronic viral infection. *Nature* **439**, 682–687, https://doi.org/10.1038/nature04444 (2006).
3. Speiser, D. E. *et al.* T cell differentiation in chronic infection and cancer: functional adaptation or exhaustion? *Nat Rev Immunol* **14**, 768–774, https://doi.org/10.1038/nri3740 (2014).
4. Pauken, K. E. & Wherry, E. J. Overcoming T cell exhaustion in infection and cancer. *Trends Immunol* **36**, 265–276, https://doi.org/10.1016/j.it.2015.02.008 (2015).
5. Wherry, E. J. & Kurachi, M. Molecular and cellular insights into T cell exhaustion. *Nat Rev Immunol* **15**, 486–499, https://doi.org/10.1038/nri3862 (2015).
6. Romo-Gonzalez, T., Chavarria, A. & Perez, H. J. Central nervous system: a modified immune surveillance circuit? *Brain Behav Immun* **26**, 823–829, https://doi.org/10.1016/j.bbi.2012.01.016 (2012).
7. Ousman, S. S. & Kubes, P. Immune surveillance in the central nervous system. *Nat Neurosci* **15**, 1096–1101, https://doi.org/10.1038/nn.3161 (2012).
8. Kipnis, J. Multifaceted interactions between adaptive immunity and the central nervous system. *Science* **353**, 766–771, https://doi.org/10.1126/science.aag2638 (2016).
9. Reardon, D. A. *et al.* Immunotherapy advances for glioblastoma. *Neuro Oncol* **16**, 1441–1458, https://doi.org/10.1093/neuonc/nou212 (2014).
10. Fecci, P. E., Heimberger, A. B. & Sampson, J. H. Immunotherapy for primary brain tumors: no longer a matter of privilege. *Clin Cancer Res* **20**, 5620–5629, https://doi.org/10.1158/1078-0432.CCR-14-0832 (2014).
11. Neagu, M. R. & Reardon, D. A. An Update on the Role of Immunotherapy and Vaccine Strategies for Primary Brain Tumors. *Current treatment options in oncology* **16**, 54, https://doi.org/10.1007/s11864-015-0371-3 (2015).
12. Tivnan, A., Heilinger, T., Lavelle, E. C. & Prehn, J. H. Advances in immunotherapy for the treatment of glioblastoma. *Journal of neuro-oncology*, https://doi.org/10.1007/s11060-016-2299-2 (2016).
13. Hellstrom, I., Hellstrom, K. E., Pierce, G. E. & Yang, J. P. Cellular and humoral immunity to different types of human neoplasms. *Nature* **220**, 1352–1354 (1968).
14. Hanson, H. L. *et al.* Eradication of established tumors by CD8+ T cell adoptive immunotherapy. *Immunity* **13**, 265–276 (2000).
15. Vuk-Pavlovic, S. Rebuilding immunity in cancer patients. *Blood cells, molecules & diseases* **40**, 94–100, https://doi.org/10.1016/j.bcmd.2007.06.025 (2008).
16. Riella, L. V., Paterson, A. M., Sharpe, A. H. & Chandraker, A. Role of the PD-1 pathway in the immune response. *American journal of transplantation: official journal of the American Society of Transplantation and the American Society of Transplant Surgeons* **12**, 2575–2587, https://doi.org/10.1111/j.1600-6143.2012.04224.x (2012).
17. Antonios, J. P. *et al.* Immunosuppressive tumor-infiltrating myeloid cells mediate adaptive immune resistance via a PD-1/PD-L1 mechanism in glioblastoma. *Neuro Oncol*, https://doi.org/10.1093/neuonc/now287 (2017).
18. Nduom, E. K. *et al.* PD-L1 expression and prognostic impact in glioblastoma. *Neuro Oncol* **18**, 195–205, https://doi.org/10.1093/neuonc/nov172 (2016).
19. Reardon, D. A. *et al.* Glioblastoma Eradication Following Immune Checkpoint Blockade in an Orthotopic, Immunocompetent Model. *Cancer Immunol Res* **4**, 124–135, https://doi.org/10.1158/2326-6066.cir-15-0151 (2016).
20. Antonios, J. P. *et al.* PD-1 blockade enhances the vaccination-induced immune response in glioma. *JCI Insight* **1**, https://doi.org/10.1172/jci.insight.87059 (2016).
21. Mathios, D. *et al.* Anti-PD-1 antitumor immunity is enhanced by local and abrogated by systemic chemotherapy in GBM. *Sci Transl Med* **8**, 370ra180, https://doi.org/10.1126/scitranslmed.aag2942 (2016).
22. Kim, J. E. *et al.* Combination Therapy with Anti-PD-1, Anti-TIM-3, and Focal Radiation Results in Regression of Murine Gliomas. *Clin Cancer Res* **23**, 124–136, https://doi.org/10.1158/1078-0432.ccr-15-1535 (2017).
23. Ampie, L., Woolf, E. C. & Dardis, C. Immunotherapeutic advancements for glioblastoma. *Front Oncol* **5**, 12, https://doi.org/10.3389/fonc.2015.00012 (2015).
24. Dunn, G. P., Old, L. J. & Schreiber, R. D. The three Es of cancer immunoediting. *Annual review of immunology* **22**, 329–360, https://doi.org/10.1146/annurev.immunol.22.012703.104803 (2004).

25. Mittal, D., Gubin, M. M., Schreiber, R. D. & Smyth, M. J. New insights into cancer immunoediting and its three component phases–elimination, equilibrium and escape. *Curr Opin Immunol* **27**, 16–25, https://doi.org/10.1016/j.coi.2014.01.004 (2014).
26. Teng, M. W., Galon, J., Fridman, W. H. & Smyth, M. J. From mice to humans: developments in cancer immunoediting. *J Clin Invest* **125**, 3338–3346, https://doi.org/10.1172/jci80004 (2015).
27. Deleidi, M., Jaggle, M. & Rubino, G. Immune aging, dysmetabolism, and inflammation in neurological diseases. *Front Neurosci* **9**, 172, https://doi.org/10.3389/fnins.2015.00172 (2015).
28. Ahmed, R., Salmi, A., Butler, L. D., Chiller, J. M. & Oldstone, M. B. Selection of genetic variants of lymphocytic choriomeningitis virus in spleens of persistently infected mice. Role in suppression of cytotoxic T lymphocyte response and viral persistence. *J Exp Med* **160**, 521–540 (1984).
29. Zhou, X., Ramachandran, S., Mann, M. & Popkin, D. L. Role of lymphocytic choriomeningitis virus (LCMV) in understanding viral immunology: past, present and future. *Viruses* **4**, 2650–2669, https://doi.org/10.3390/v4112650 (2012).
30. Scott-Browne, J. P. *et al*. Dynamic Changes in Chromatin Accessibility Occur in CD8+ T Cells Responding to Viral Infection. *Immunity* **45**, 1327–1340, https://doi.org/10.1016/j.immuni.2016.10.028 (2016).
31. Crawford, A. *et al*. Molecular and transcriptional basis of CD4(+) T cell dysfunction during chronic infection. *Immunity* **40**, 289–302, https://doi.org/10.1016/j.immuni.2014.01.005 (2014).
32. Penaloza-MacMaster, P. *et al*. Interplay between regulatory T cells and PD-1 in modulating T cell exhaustion and viral control during chronic LCMV infection. *J Exp Med* **211**, 1905–1918, https://doi.org/10.1084/jem.20132577 (2014).
33. Im, S. J. *et al*. Defining CD8+ T cells that provide the proliferative burst after PD-1 therapy. *Nature* **537**, 417–421, https://doi.org/10.1038/nature19330 (2016).
34. Zitvogel, L., Pitt, J. M., Daillere, R., Smyth, M. J. & Kroemer, G. Mouse models in oncoimmunology. *Nat Rev Cancer* **16**, 759–773, https://doi.org/10.1038/nrc.2016.91 (2016).
35. Singer, M. *et al*. A Distinct Gene Module for Dysfunction Uncoupled from Activation in Tumor-Infiltrating T Cells. *Cell* **166**, 1500–1511.e1509, https://doi.org/10.1016/j.cell.2016.08.052 (2016).
36. Duraiswamy, J., Freeman, G. J. & Coukos, G. Therapeutic PD-1 pathway blockade augments with other modalities of immunotherapy T-cell function to prevent immune decline in ovarian cancer. *Cancer Res* **73**, 6900–6912, https://doi.org/10.1158/0008-5472.can-13-1550 (2013).
37. Oh, T. *et al*. Immunocompetent murine models for the study of glioblastoma immunotherapy. *J Transl Med* **12**, 107, https://doi.org/10.1186/1479-5876-12-107 (2014).
38. Chamberlain, M. C. & Kim, B. T. Nivolumab for patients with recurrent glioblastoma progressing on bevacizumab: a retrospective case series. *Journal of neuro-oncology*, https://doi.org/10.1007/s11060-017-2466-0 (2017).
39. Blattman, J. N. *et al*. Estimating the precursor frequency of naive antigen-specific CD8 T cells. *J Exp Med* **195**, 657–664 (2002).
40. Malandro, N. *et al*. Clonal Abundance of Tumor-Specific CD4(+) T Cells Potentiates Efficacy and Alters Susceptibility to Exhaustion. *Immunity* **44**, 179–193, https://doi.org/10.1016/j.immuni.2015.12.018 (2016).
41. Klein, L. *et al*. Visualizing the course of antigen-specific CD8 and CD4 T cell responses to a growing tumor. *Eur J Immunol* **33**, 806–814, https://doi.org/10.1002/eji.200323800 (2003).
42. Odorizzi, P. M., Pauken, K. E., Paley, M. A., Sharpe, A. & Wherry, E. J. Genetic absence of PD-1 promotes accumulation of terminally differentiated exhausted CD8+ T cells. *J Exp Med* **212**, 1125–1137, https://doi.org/10.1084/jem.20142237 (2015).
43. Fuertes Marraco, S. A., Neubert, N. J., Verdeil, G. & Speiser, D. E. Inhibitory Receptors Beyond T Cell Exhaustion. *Front Immunol* **6**, 310, https://doi.org/10.3389/fimmu.2015.00310 (2015).
44. Sen, D. R. *et al*. The epigenetic landscape of T cell exhaustion. *Science* **354**, 1165–1169, https://doi.org/10.1126/science.aae0491 (2016).
45. Brown, K. E., Freeman, G. J., Wherry, E. J. & Sharpe, A. H. Role of PD-1 in regulating acute infections. *Curr Opin Immunol* **22**, 397–401, https://doi.org/10.1016/j.coi.2010.03.007 (2010).
46. Allie, S. R., Zhang, W., Fuse, S. & Usherwood, E. J. Programmed death 1 regulates development of central memory CD8 T cells after acute viral infection. *J Immunol* **186**, 6280–6286, https://doi.org/10.4049/jimmunol.1003870 (2011).
47. Dronca, R. S. *et al*. T cell Bim levels reflect responses to anti-PD-1 cancer therapy. *JCI Insight* **1**, https://doi.org/10.1172/jci.insight.86014 (2016).
48. Wheeler, L. A. *et al*. Phase II multicenter study of gene-mediated cytotoxic immunotherapy as adjuvant to surgical resection for newly diagnosed malignant glioma. *Neuro Oncol* **18**, 1137–1145, https://doi.org/10.1093/neuonc/now002 (2016).
49. Mangani, D., Weller, M. & Roth, P. The network of immunosuppressive pathways in glioblastoma. *Biochemical pharmacology* **130**, 1–9, https://doi.org/10.1016/j.bcp.2016.12.011 (2017).
50. Kamphorst, A. O. *et al*. Rescue of exhausted CD8 T cells by PD-1-targeted therapies is CD28-dependent. *Science* **355**, 1423–1427, https://doi.org/10.1126/science.aaf0683 (2017).
51. Pauken, K. E. *et al*. Epigenetic stability of exhausted T cells limits durability of reinvigoration by PD-1 blockade. *Science* **354**, 1160–1165, https://doi.org/10.1126/science.aaf2807 (2016).
52. Utzschneider, D. T. *et al*. T cells maintain an exhausted phenotype after antigen withdrawal and population reexpansion. *Nat Immunol* **14**, 603–610, https://doi.org/10.1038/ni.2606 (2013).
53. Schumacher, T. *et al*. A vaccine targeting mutant IDH1 induces antitumour immunity. *Nature* **512**, 324–327, https://doi.org/10.1038/nature13387 (2014).
54. Eckel-Passow, J. E. *et al*. Glioma Groups Based on 1p/19q, IDH, and TERT Promoter Mutations in Tumors. *N Engl J Med* **372**, 2499–2508, https://doi.org/10.1056/NEJMoa1407279 (2015).
55. Wherry, E. J. *et al*. Molecular signature of CD8+ T cell exhaustion during chronic viral infection. *Immunity* **27**, 670–684, https://doi.org/10.1016/j.immuni.2007.09.006 (2007).
56. Giordano, M. *et al*. Molecular profiling of CD8 T cells in autochthonous melanoma identifies Maf as driver of exhaustion. *Embo j* **34**, 2042–2058, https://doi.org/10.15252/embj.201490786 (2015).
57. Nakashima, H., Nguyen, T., Goins, W. F. & Chiocca, E. A. Interferon-stimulated gene 15 (ISG15) and ISG15-linked proteins can associate with members of the selective autophagic process, histone deacetylase 6 (HDAC6) and SQSTM1/p62. *J Biol Chem* **290**, 1485–1495, https://doi.org/10.1074/jbc.M114.593871 (2015).
58. Seyfried, T. N., el-Abbadi, M. & Roy, M. L. Ganglioside distribution in murine neural tumors. *Molecular and chemical neuropathology* **17**, 147–167 (1992).

Acknowledgements

Thanks to Michelle Lifton of the CVVR Flow cytometry core in BIDMC for experimental assistance, to the NIH tetramer core facility for the GP33 tetramer material, to Eric McLaughlin for help in statistical analyses, and to Sylwia Wojcik for the crucial lab managing work in the HCNL labs. E.A.C. was supported by NCI grants, P01CA163205 and P01CA069246, P.P.M. by NIH grant 1K22 AI118421, the Institutional Research Grant, IRG-15-173-21 from the American Cancer Society and the Chicago Third Coast CFAR grant P30 AI117943, G.J.F. by P50CA101942.

Author Contributions

H.N. conceived the project and designed the experiments, conducted the experiments and interpreted the data. Q.A.A. and P.P.M. contributed by performing some of the experiments and generated the manuscript figures. S.F. supervised statistical analyses. H.N. and E.A.C. supervised and wrote the manuscript. P.P.M., G.J.F., V.K.K., D.A.R. and M.C. provided analyses, suggestions and comments.

Additional Information

Supplementary information accompanies this paper at https://doi.org/10.1038/s41598-017-18540-2.

Competing Interests: G.F. has patents/pending royalties on the PD-1 pathway. Other authors declare no potential conflicts of interest.

Publisher's note: Springer Nature remains neutral with regard to jurisdictional claims in published maps and institutional affiliations.